Clays and Clay Minerals, Vol. 66, No. 5, 415–425, 2018.

IRON-PILLARED MONTMORILLONITE AS AN INEXPENSIVE CATALYST FOR 2-NITROPHENOL REDUCTION

HONGHAI WU*, ZHENHAO SONG, MEIXIANG LV, DAN ZHAO, AND GUANGPING HE

Key Laboratory of Theoretical Chemistry of Environment, Ministry of Education; School of Chemistry and Environment, South China Normal University, Guangzhou 510006, China

Abstract—Many types of oxidative pollutants are dangerous chemicals and may pose a health risk, but an inexpensive and effective method for mitigating those risks would offer significant advantages. The objective of this study was, therefore, to investigate the potential for Fe-pillared montmorillonite to fill that gap. Surface mediated reduction reactions by ferrous species often play an important role in governing the transport, transformation, and fate of hazardous oxidative contaminants. Compared to the untreated montmorillonite (Mnt), the synthetic polyhydroxyl-Fe pillared montmorillonite (Fe-Mnt) was found to be somewhat similar to goethite in promoting the ability of specifically adsorbed Fe(II) to reductively transform 2-nitrophenol (2-NP). The 2-NP was efficiently removed within 30 min from solutions at the optimum neutral pH in a mixed reduction system of Fe(II)/Fe-Mnt under an anoxic atmosphere. This demonstrated that the specifically adsorbed Fe(II) of Fe-Mnt can enhance 2-NP reduction. The highly enhanced 2-NP reduction by Fe(II) through Fe-Mnt surface catalysis can, therefore, be ascribed to clearly increased amounts of an adsorbed Fe(II) species surface complex, which gave rise to enhanced Fe(II) reductive activity that enabled the rapid reduction of 2-NP. The reduction processes produced a faster transformation of 2-NP in a Fe-Mnt suspension than in a Mnt suspension. The transformation kinetics were described using pseudo-first-order rate equations. Moreover, in addition to the effects of mineral surface properties, the interactions were affected by the aqueous chemistry, and the removal rates of 2-NP were increased at pHs of 6.0−7.3. In the present study, the structure and surface reactivity of Fe-Mnt was characterized in depth. The polyhydroxyl-Fe added to Mnt and the pH were determined to be the two key controlling factors to mediate the reductive transformation of 2-NP in the presence of Fe-Mnt in comparison to goethite and Mnt. Finally, the catalysis mechanism responsible for the enhanced 2-NP reduction by Fe(II) was elucidated using cyclic voltammetry.

Key Words—2-Nitrophenol, Ferrous Iron, Fe-pillared Montmorillonite, Reductive Transformation, Surface Catalysis.

INTRODUCTION

Iron is known to be the most abundant transition metal in the Earth's crust and it has three major valence states: zero-valent Fe, ferrous [Fe(II)], and ferric [Fe(III)]. Wetland and aquifer sediments are anoxic environments that often contain high levels of Fe(II) in pore waters (Klupinski *et al*., 2004). The Fe(II) species specifically adsorbed to mineral surfaces can often enable diverse oxidative contaminants to be reductively transformed easily (Elsner *et al*., 2004). Under anoxic conditions, chemical (*i.e*., abiotic) reactions that occur at mineral surfaces can contribute significantly to the reductive degradation of oxidative contaminants, which can include well-documented organic compounds, such as halogenated methanes and nitroaromatic compounds (NACs), as well as high-valence toxic metals, *e.g.* Tc(VII), U(VI), and Cr(VI). Hence, studies on the interactions between the Fe(II) species and mineral surfaces have attracted attention and have been aimed to obtain insights into the surface catalysis mechanisms that are responsible for promoting pollutant reduction by the surface association of Fe(II) species in the environment (Stumm and Sulzberger, 1992; Klupinski *et al*., 2004; Zhang *et al*., 2017).

The redox potential (E_h) of Fe(III)/Fe(II) can be decreased considerably when ferrous species are specifically adsorbed to the surfaces of diverse ferric (oxyhydr)oxides (hereafter referred to as ferric oxide) (Klausen *et al*.,1995) and is also found on TiO_2 and Al_2O_3 surfaces. The E_h decrease, however, is not evident on the surfaces of montmorillonite (Mnt), which is ubiquitous in soils and sediments. These research efforts have proved that oxide surfaces can provide much greater amounts of surface Fe hydroxyls to stabilize Fe(II) by the formation of surface complex Fe(II) species, *e.g.* $\equiv SOFe^{+}$, $\equiv SOFeOH^{0}$, and $\equiv SOFeO^{-}$. These surface complex Fe(II) species have a lower E_h in comparison to aqueous Fe(II) (Li *et al*., 2009). As a result, Fe(II) species can be more easily oxidized through surface catalysis by oxides than by clay minerals. Previous studies further concluded that an increased amount of Fe(II) in surface complexes is a necessary condition for the effective reduction of pollutants (Hoffstetter *et al*., 1999; Strathmann and Stone, 2002; Borch *et al*., 2005; Tao *et al*., 2010; Tao *et*

* E-mail address of corresponding author:
whh302@163.com
DOI: 10.1346/CCMN.2018.064107

al, 2012; Jones *et al*., 2016). The cycling of Fe(III)/Fe(II), therefore, often plays an important role in mediating interface redox reactions, where the Fe(II) species usually participate in the reduction of many oxidative pollutants. The adsorption behavior of Fe(II) species to minerals, however, has been shown to depend on the nature of the mineral surfaces (involved groups and charges) and even on the mineral bulk structures.

Because natural montmorillonite basal surfaces have most of the high negative charge density, the amount of Fe(II) surface complexes bound to edge surfaces is much lower than the exchangeable Fe(II) bound to basal surfaces and results in a weaker transformation of 2-nitrophenol by natural Mnt.

Mnt is quite different from goethite in promoting 2-NP reduction by Fe(II) because Mnt has a high capacity to adsorb Fe(II). No E_h improvement has been observed, however, for Mnt with cation exchanged Fe(II) in comparison to aqueous Fe(II). Attempts have been made to increase the amount of Fe(II) adsorbed to minerals *via* surface complexation by increasing solution pH and/or aqueous Fe(II) concentrations in most reduction reaction systems (Strathmann and Stone, 2002; Li *et al*., 2008).

On the other hand, polyhydroxyl Fe(III) species added to clay mineral surfaces can actually be used to fabricate various Fe-oxide and phyllosilicate mixtures that are similar to what naturally occurs during soil formation. More importantly, the polyhydroxyl Fe(III) oxides added to clay minerals during the modification process can provide much higher contents of surface Fe hydroxyl groups on clay mineral surfaces. In addition to the mineral Fe(II) surface complex, the structural Fe(II) in clay minerals also obviously exerts reductive reactivity (Pentráková *et al*., 2013; Brookshaw *et al*., 2014), albeit the activity is somewhat lower than Fe(II) surface complex species. The reductive activity of structural Fe(II) in most iron-bearing minerals, *e.g.* Mnt, vermiculite, and biotite, may be weakened to a certain extent due to slow electron transfer in the bulk mineral. Currently, many contaminated sites need to be remediated, which demands the development of cost-effective techniques to efficiently dispose of oxidative pollutants (Haderlein and Schwarzenbach, 1995).

The objective of the present study was to evaluate how the introduction of polyhydroxyl-Fe(III) species affects the reductive catalytic activity of mineral surfaces to promote the reductive ability of Fe(II). As expected, the polyhydroxyl-Fe(III) modification of Mnt was found to be an effective method to enhance the surface Fe(II) catalytic activity of Fe-Mnt. Mnt was chosen to investigate the potential of polyhydroxyl-Fe(III) species to effectively improve the reductive catalytic activity of clay minerals. Therefore, a polyhydroxyl-Fe(III) pillared Mnt (Fe-Mnt) was synthesized *via* the introduction of a polyhydroxyl-Fe(III) species into an Mnt sample. The Fe-pillaring modification enabled the resultant Fe-Mnt to increase the adsorption capacity for an Fe(II) surface complex by decreasing the negative charge density of the Mnt surfaces and by increasing the number of surface Fe oxide hydroxyls. Finally, the aims of the present study were to explore the significance of Fe-Mnt as a Fe(II) catalyst to promote the efficient reduction of 2-NP as a probe compound and to elucidate the mechanism of the enhanced catalytic reduction of 2-NP using electrochemical methods.

MATERIALS AND METHODS

Chemicals and reaction solutions

Montmorillonite was supplied by the Zhejiang Sanding Technology Co. Ltd. (Zhejiang, China). Both the Fe-pillared montmorillonite and goethite samples were synthesized. The 3-(N-morpholino)propanesulfonic acid ($C_7H_{15}NO_4S$, MOPS, 99.0% purity for pHs >7, 2-(N-morpholino)ethanesulfonic acid monohydrate ($C_6H_{13}NO_4S{\cdot}H_2O$, MES, 99.0% for pHs <7), and 2-nitrophenol (2-NP, 99.5% purity) were purchased from the Aladdin Reagent Factory (Shanghai, China). Other chemicals, which included $FeSO_4{\cdot}7H_2O$, $Fe(NO_3)_3{\cdot}9H_2O$, Na_2CO_3, NaOH, HCl, NaCl, and methanol (HPLC), were all purchased from the Tianjin Chemical Reagent factory (Tianjin, China). All chemicals were of analytical grade and were used without further purification. Oxidation of the Fe(II) stock solution ($FeSO_4$) was minimized by acidifying the solution with 0.2 M HCl. The solution was then filtered through a 0.45 μm membrane and kept at approximately 1.25 M Fe.

Preparation of Fe-pillared montmorillonite and goethite

The synthetic Fe-pillared montmorillonite (Fe-Mnt) was prepared using the method described by Yuan *et al*. (2008). Na_2CO_3 powder (5.3 g) was slowly added to an aqueous solution (250 mL) of 0.2 mol/L $Fe(NO_3)_3$ with vigorous stirring for 2 h. The translucent red-brown pillaring solution (A) was aged for 24 h at room temperature and then a 200 mL portion was added to a 20 g/L Mnt suspension (200 mL) at a rate of 10 mL/min under vigorous stirring at 60ºC to give the desired [Fe]/Mnt ratio of 10 mmol/g. The obtained mixture was stirred for 2 h and aged for 24 h at 60ºC. Then, the solid product was successively centrifuged and washed several times with deionized water. The resultant wet cake was air dried at 80ºC to produce the Fe-pillared Mnt. The same synthesis method was repeated using 100 and 300 mL of A to achieve [Fe]/Mnt ratios in the suspensions of 5.0 and 15.0 mmol/g, respectively. The samples with 5.0, 10.0, and 15.0 mmol/g ratios were denoted Fe-Mnt1, Fe-Mnt2, and Fe-Mnt3, respectively. The chemical compositions of the Mnt and Fe-Mnt samples were analyzed using a PANalytical PW-4400 X-ray (PANalytical, Amelo, The Netherlands) fluorescence spectrometer (XRF) (Table 1). Goethite was synthesized

https://doi.org/10.1346/CCMN.2018.064107 Published online by Cambridge University Press

using the method reported by Wu *et al*. (2012). The Fe-Mnt catalyst samples were pulverized to pass through a 200-mesh sieve before use.

Characterization of the mineral catalysts

Powder X-ray diffraction patterns (XRD) of the Mnt and Fe-Mnt samples were determined using a Bruker D8 ADVANCE X-ray diffractometer (Bruker, Karlsruhe, Germany) with Cu Kα radiation. The high-resolution transmission electron microscopy (HRTEM) images were obtained using a JEOL JEM 2100HR (JEOL, Tokyo, Japan) operated at an accelerating voltage of 200 kV. The Fourier-transform infrared spectra (FTIR) were recorded using a Nicolet 6700 FTIR spectrometer (Thermo Scientific, Madison, Wisconsin, USA). The Brunauer-Emmett-Teller (BET) specific surface areas and Barrett-Joyner-Halenda (BJH) sample pore sizes and pore volumes were measured using an ASAP 2020 gas adsorption analyzer (Micromeritics, Norcross, Georgia, USA). These analysis methods were described in a previous report (Wu *et al*., 2016). The sample zeta potentials were measured using a Nano ZS90 nanosize zeta potential analyzer (Malvern Panalytical, Westborough, Massachusetts, USA). The particle size distribution of the Mnt sample was determined using the cumulant method of dynamic light scattering (DLS) analysis from data collected at a 90º scattering angle using the Nano ZS90 analyzer.

Electrochemical Tests

Cyclic voltammograms (CVs) were measured using the methods described in Li *et al*. (2009). In brief, three glassy C (GC) electrodes modified with minerals were prepared by coating bare GC electrodes with Mnt, Fe-Mnt, or goethite (Gth). Prior to the coating with minerals, the GC electrodes were successively polished using emery paper, 0.5 μm Al_2O_3 powder, and 0.05 μm Al_2O_3 powder. The GC electrodes were rinsed with deionzed water in an ultrasonic bath for 3 min after each polishing step. Then, the GC electrodes were further cleaned with acetone followed by water in an ultrasonic bath for 10 min. Meanwhile, 4 μL of each Mnt, Fe-Mnt, and goethite slurry (that contained 5 mg of mineral) was prepared in a dilute Nafion (ionic fluoropolymer-copolymer based on sulfonated tetrafluoroethylene) solution (0.5 wt.%, 250 μL) to coat each GC electrode. The mineral coated electrodes were then dried in air for 30 min. The three GC electrodes modified with the mineral coatings were identified as Mnt/GC, Fe-Mnt/GC, Gth/GC, and the bare GC electrode was identified simply as GC. Electrochemical measurements were conducted using a classical three electrode cell, where Mnt/GC, Fe-Mnt/GC, and Gth/GC were used as the working electrodes for each test. A Pt spiral was used as the counter electrode and a saturated calomel electrode (SCE) was used as the reference electrode of +0.24 V *vs.* the standard hydrogen electrode (SHE) at 25ºC. The CVs were recorded using a PGSTAT 30 Autolab potentiostat (Metrohm/Eco Chemie, Utrecht, The Netherlands) using a scan rate of 50 mV/s under an N_2 atmosphere.

Reduction kinetics experiments

The kinetics of 2-NP reduction by Fe(II) was measured in batch experiments performed under anaerobic atmospheric conditions using high purity N_2 at various pHs. The 2-NP reduction experiments were conducted in an aqueous suspension in a 250-mL glass reactor sealed with a plastic membrane. The suspensions contained 0.2 M NaCl, 28 mM buffer (MOPS or MES), 22 μM 2-NP, 3.0 mM $FeSO_4$, and 4.0 g/L of each mineral catalyst sample. The Fe(II) adsorption was allowed to proceed for 2 h prior to the addition of 2-NP into the suspensions. Once the 2-NP was added to the suspensions, the 2-NP reduction reaction started. The reactor was placed on a shaker in the dark with agitation at 400 revolutions/min and was maintained at a constant temperature. Then, at certain time intervals, 2.0 mL aliquots of the suspensions were sampled, to which 2.0 M HCl (<20 μL) was added to quench the reactions. This was followed by filtration through a 0.45 μm PTFE filter prior to analysis to measure the 2-NP concentrations.

Analytical methods

The concentrations of 2-NP were quantified using high-performance liquid chromatography (HPLC) with a Shimadzu LC-10AT (Shimadzu, Suzhou, China) HPLC with a UV detector (SPD-10AV). A Syncronis C18 column (ANPEL, Shanghai, China) (5 m, 250 mm long, and 4.6 mm in diameter) was used as the stationary phase. The isocratic mobile phase for 2-NP determination was a 70/30 (V/V) mixture of methanol/ultrapure water (pH = 2.8) at a 1.0 mL/min flow rate at 25ºC with detection at 265 nm. Using the spectrophotometric method, the concentrations of Fe(II) were analyzed using a

Table 1. Compositions of Mnt and Fe-Mnt determined using X-ray fluorescence analysis.

Oxides(%)	SiO_2	Fe_2O_3	Al_2O_3	CaO	MgO	K_2O	TiO_2	Na_2O
Mnt	66.25	3.04	21.35	2.95	2.82	0.82	0.13	2.63
Fe-Mnt1	52.34	14.72	14.75	1.07	1.51	0.32	0.05	0.21
Fe-Mnt2	47.42	36.11	13.88	0.11	1.79	0.57	0.10	0.02
Fe-Mnt3	38.88	45.84	11.28	0.08	2.01	0.72	0.18	0.22

https://doi.org/10.1346/CCMN.2018.064107 Published online by Cambridge University Press

UV-7502PCS UV-vis spectrophotometer (JINGKE, Shanghai, China) with detection at λ = 510 nm (Wei *et al*., 2017). The removal efficiency (η) of 2-NP *via* reduction can be calculated using the following equation:

$$\eta\ (\%) = 100(C_0 - C)/C_0 \quad (1)$$

where C_0 and C_t (mmol/L) are the initial and time-dependent concentrations of 2-NP, respectively. To confirm the repeatability of the experimental data, the reduction reactions were carried out in duplicate to obtain standard deviations (P) ⩽ 5%.

RESULTS AND DISCUSSION

Catalyst characterization using XRD, N_2 adsorption–desorption isotherms, TEM, and FTIR

X-ray diffraction (XRD) patterns of the natural raw montmorillonite (Mnt) and the synthetic Fe-pillared montmorillonite (Fe-Mnt) were reported by Wu *et al*. (2016). The two strong reflections observed at 2θ = 7.26º (001) and 19.88º (02, 11) were attributed to the predominant Na-montmorillonite (Na-Mnt) component found in the Mnt sample (Figure 1). The major (001) reflection shifted from a 2θ value of 7.26º to 5.65º, which corresponds to a basal spacing increase from d_{001} = 1.25 to 1.55 nm. Meanwhile, the (001) reflection intensity of Fe-Mnt was weakened to some extent, which indicates that the Na-Mnt counterpart in Fe-Mnt was successfully intercalated with the polyhydroxyl-Fe(III) oxides. No discernible reflections from any crystalline Fe (oxyhydr)oxide phase were present in Fe-Mnt because such phases have a substantially lower degree of crystallinity. Some impurity phases, such as calcite and quartz, were also identified in the Mnt sample, whereas calcite in the Fe-Mnt sample disappeared after acid dissolution, but quartz and cristobalite remained.

The N_2 adsorption isotherms of both Mnt and Fe-Mnt were assigned to type IV in the traditional classification of Brunauer, Deming, Deming, and Teller (Brunauer *et al*., 1940; Wu *et al*., 2016). As seen in Figure 2, the enlarged hysteresis loop and predominant small mesopores in the pore size distribution clearly indicate that Fe-Mnt is a mesoporous material. The Fe-Mnt sample had a relatively wide pore size distribution with a consequent increase in the number of micropores, which led to a higher pore volume and a smaller average pore size (Table 2). The BET surface area of Fe-Mnt increased relative to Mnt. These results revealed that polyhydroxyl-Fe was successfully pillared into the Na-Mnt phase to form microporous structures in Fe-Mnt. In addition, the measured average particle size of the Mnt sample was 737 nm, which is smaller than the 1108 nm measured for the Fe-Mnt sample.

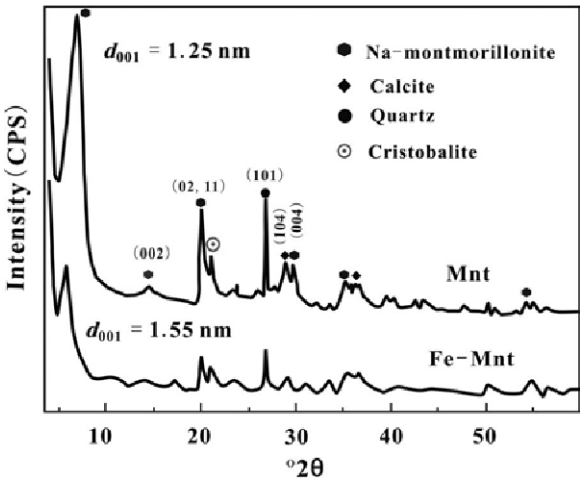

Figure 1. XRD patterns of Mnt and Fe-Mnt.

Face-to-edge contact between the Na-Mnt particles was found with a random orientation to form the traditional "card-house structure" in the raw Mnt sample (Figure 3a). Meanwhile, Fe-Mnt clearly formed a typical delaminated structure, which was described in a previous study (Yuan *et al*., 2008). In the Fe-Mnt sample, many small dark particles that correspond to amorphous Fe oxide aggregates were clearly found that were randomly distributed on the surfaces of the Na-Mnt phase particles (Figure 3b). With the pillaring and/or the partial surface coverage by the polyhydroxyl-Fe species, the specific surface areas and pore volumes of Fe-Mnt were drastically increased relative to Mnt due to the formation of delaminated structures in Fe-Mnt.

The FTIR spectra of the Mnt and Fe-Mnt samples (Figure 4) were consistent with previously reported results (Wu *et al*., 2016). The characteristic band in the –OH stretching region (3626 cm^{-1}) corresponds to the Al–O–H group while the band at approximately 1038 cm^{-1} was ascribed to Si–O–Si stretching. Two bands centered at 468 and 524 cm^{-1} in the raw Mnt sample were the stretching modes of Si–O–Fe and Si–O–Al, respectively. The two bands in Fe-Mnt were slightly shifted while the 1038 cm^{-1} peak of Na-Mnt was shifted to 1040 cm^{-1} after the Fe-pillaring modification. One new peak centered at 1384 cm^{-1}, however, was clearly found in the FTIR spectra of Fe-Mnt and was ascribed to NO_3^- stretching (Yuan *et al*., 2008). This indicates that Fe-Mnt has positively charged surfaces that were generated by the successful introduction of the polyhydroxyl-Fe species. The disappearance of the 3626 cm^{-1} peak and the simultaneous appearance

Table 2. Structural and surface parameters of Mnt and Fe-Mnt.

Mineral materials	Surface area (m^2/g)	Pore volume (cm^3/g)	Average pore size (nm)
Mnt	15.2	0.047	6.17
Fe-Mnt-2	112.3	0.100	3.55

https://doi.org/10.1346/CCMN.2018.064107 Published online by Cambridge University Press

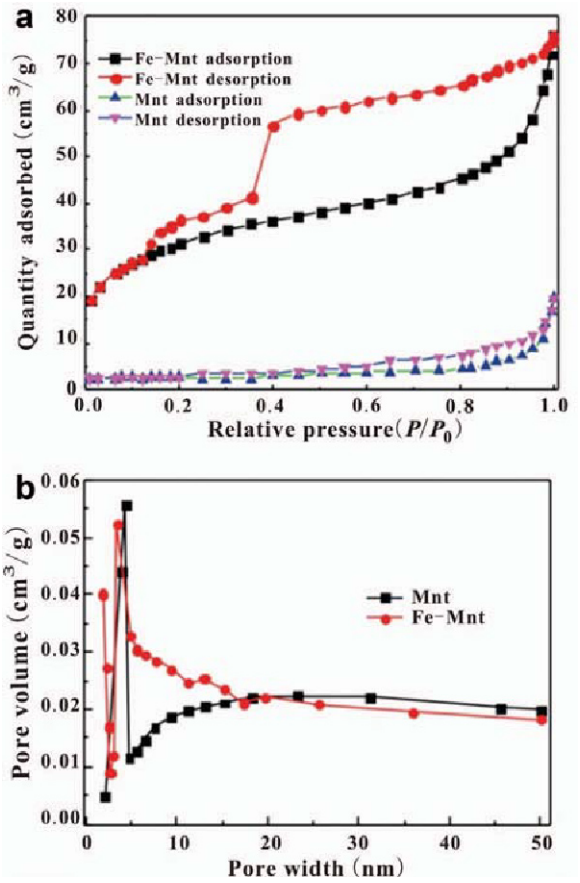

Figure 2. Nitrogen adsorption–desorption isotherms of Mnt and Fe-Mnt; BJH pore size distributions of (a) Mnt and (b) Fe-Mnt.

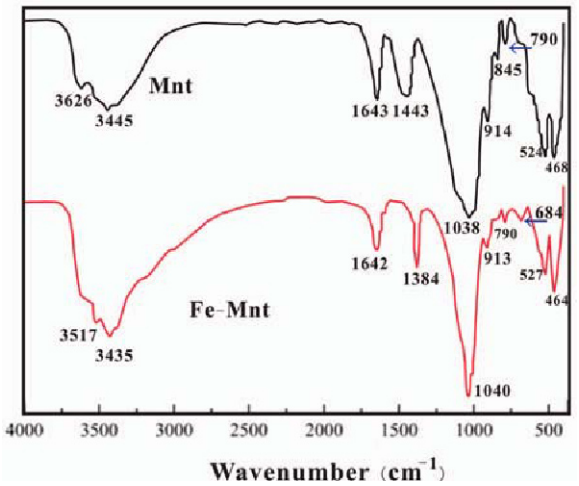

Figure 4. FTIR spectra of Mnt and Fe-Mnt.

of new bands at 3435 or 3517 cm^{-1} all mean that several different forms of bound water were generated by polyhydroxyl-Fe adsorption to Fe-Mnt.

Several kinetic reaction processes for 2-NP removal

The 2-NP removal efficiencies measured in Mnt and Fe-Mnt suspensions without any added Fe(II) ions were approximately 20% (Figure 5). The low removal efficiencies may be ascribed to removal just by adsorption of 2-NP to the two mineral materials and this implies that Mnt is similar to Fe-Mnt with regard to 2-NP surface adsorption. On the other hand, a 2-NP removal efficiency of approximately 50% was obtained for an homogeneous reduction system with aqueous Fe(II) species. For the heterogeneous reduction systems at pH 6.7, the Fe(II)/Mnt system reductively removed approximately 85% of 2-NP within 4 h, while the Fe(II)/Fe-Mnt system almost entirely reduced the added 2-NP within 0.5 h.

The above results demonstrate that Fe-Mnt was more efficient than Mnt in the catalyzed reduction of 2-NP by Fe(II). As expected, goethite had the strongest surface reductive catalytic activity for Fe(II) and the highest reductive removal efficiency for 2-NP that can be reached even at pH = 6.3 in the Fe(II)/goethite system (Figure 5), which almost approaches that obtained in the Fe(II)/Fe-Mnt system at pH = 6.7. These results illustrate that Fe oxide surfaces can greatly affect the reductive removal of 2-NP. As such, the Fe content of Fe-Mnt may be another key mediating factor in addition to the solution pH values.

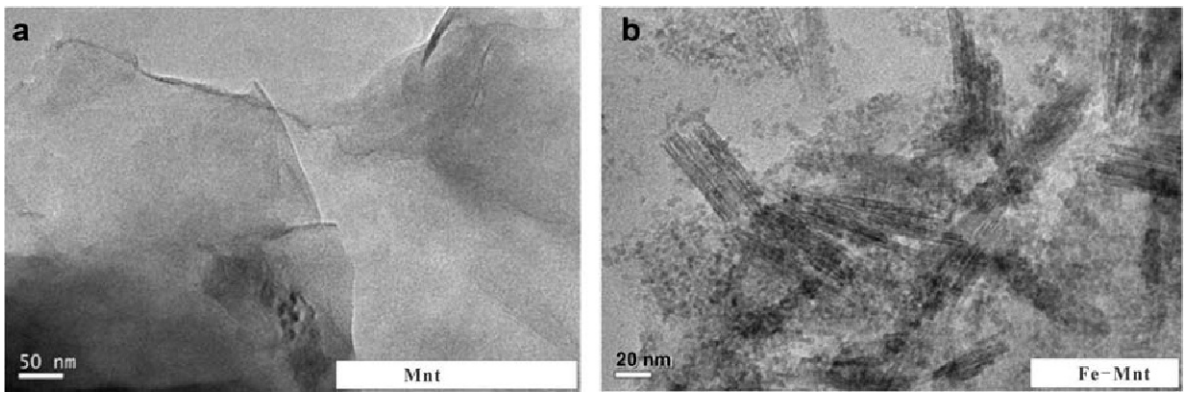

Figure 3. TEM images of (a) Mnt and (b) Fe-Mnt.

https://doi.org/10.1346/CCMN.2018.064107 Published online by Cambridge University Press

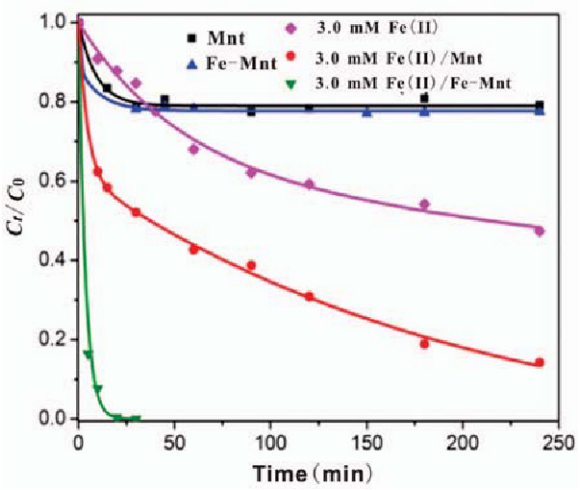

Figure 5. The 2-NP removal rates in several different reduction systems under the initial conditions of 22 μM 2-NP, 4.0 g/L of each catalyst, pH 6.7, 0.2 M NaCl, 28 mM MOPS, 3.0 mM Fe(II), and 25ºC.

Effects of iron(III) added to Fe-Mnt

The Fe(III) content in Fe-Mnt can affect the kinetics of 2-NP reductive removal (Figure 6). Increased amounts of Fe added to Fe-Mnt promoted an increase in the 2-NP removal efficiency. The 2-NP removal efficiencies only increased slightly, however, when the Fe/Mnt ratio was changed from 10.0 mg/g to 15.0 mg/g. The Fe/Mnt mass ratio of 10.0 mg/g corresponded to sample Fe-Mnt2, which was chosen for a subsequent exploration of the catalytic reduction mechanisms.

Effect of pH

The solubility product constants (K_{sp}) of $Fe(OH)_2$ and $Fe(OH)_3$ are 1.0×10^{-15} and 3.2×10^{-38} (Dai, 2006), respectively. When the aqueous Fe(II) concentration is 3.0 mmol/L, no $Fe(OH)_2$ precipitates at pHs <7.5. Apparently, in the 5.5 to 7.3 pH range, the Fe(II) species bind to the minerals by adsorption only. If 3.0 mmol/L Fe(II) is completely oxidized into Fe(III), $Fe(OH)_3$ will possibly precipitate at pHs >2.3.

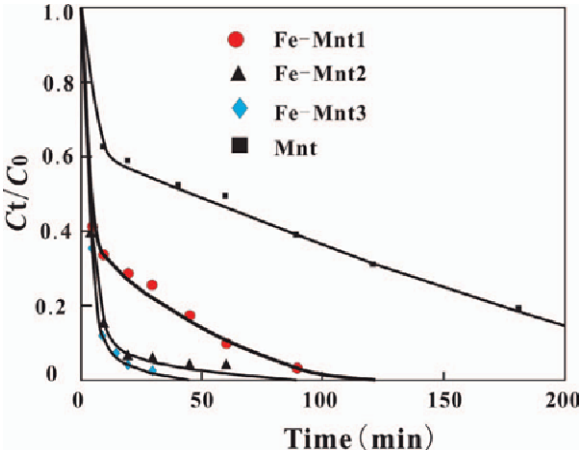

Figure 6. Effect of the Fe content added to Fe-Mnt on 2-NP transformation rates at pH 6.5 with other initial conditions the same as specified in Figure 5.

The adsorptive removal rates for 2-NP by the minerals were independent of pH (Figure 5), but the rates of 2-NP reductive removal from the mineral catalyzed Fe(II) reduction systems increased with increases in pH (Figure 7). In the case of the Fe(II)/Mnt mixed reduction system, the reduction process gave a much lower removal rate for 2-NP at pH 6.0, whereas the maximum removal rate for 2-NP in the same reduction system was reached at pH 7.3, which is higher than that for the Fe(II)/Fe-Mnt mixed system described below.

Due to the introduction of polyhydroxyl-Fe(III) oxides into the Mnt particles, the effective pH value was 6.0 for Fe-Mnt, which is much lower than the pH 6.7 of Mnt, but still higher than the pH 5.5 of goethite (Gth). As a result, the desired effective pH to start the reduction of 2-NP by Fe(II) decreased with increases in the catalyst Fe content in the following order at the effective pH values: Gth < Fe-Mnt < Mnt. This clearly demonstrates that the nature of the mineral surfaces can greatly affect the reductive ability of the Fe(II) surface complex species and also indicates that polyhydroxyl Fe(III) pillaring allowed the synthetic Fe-Mnt catalyst to partially form Fe-oxide-like reactive surfaces.

The pH_{iep} values of the selected three mineral materials were 2.1, 3.8, and 8.2 for Mnt, Fe-Mnt2, and Gth, respectively (Figure 8). The zeta potentials for the Fe-Mnt2 sample were still negative when the tested pHs were >3.8. As expected, the introduction of polyhydroxyl-Fe(III) oxides into Mnt changed the surface charge of the Fe-Mnt that was formed. The negative surface charge densities of minerals usually increase with increases in the pH. The well-recognized conclusion drawn from these results is that surface hydroxyls on minerals can be deprotonated as the pH increases and the negative deprotonated surface sites generated are always beneficial to Fe(II) coordination to mineral surfaces (Schultz and Grundl, 2000). Moreover, an Fe(II) surface complex can enable easy electron transfer from Fe(II) to the mineral surfaces. Hence, similar to 4-chloro-1-nitrobenzene ($C_6H_4ClNO_2$) reduction (Schultz and Grundl, 2000), the efficient reduction of 2-NP required a high pH of 7.3 for the Fe(II)/Mnt mixed system.

Electrochemical evidence

All voltammograms clearly exhibited a pair of peaks (Figure 9): (1) an anodic oxidation peak for Fe(II) at potentials that ranged from −0.2 to 0.4 V (*vs.* SCE, all voltages reported below are in reference to SCE); and (2) a cathodic reduction peak for Fe(III) at potentials that ranged from −0.6 to −0.1 V. The peak oxidation

https://doi.org/10.1346/CCMN.2018.064107 Published online by Cambridge University Press

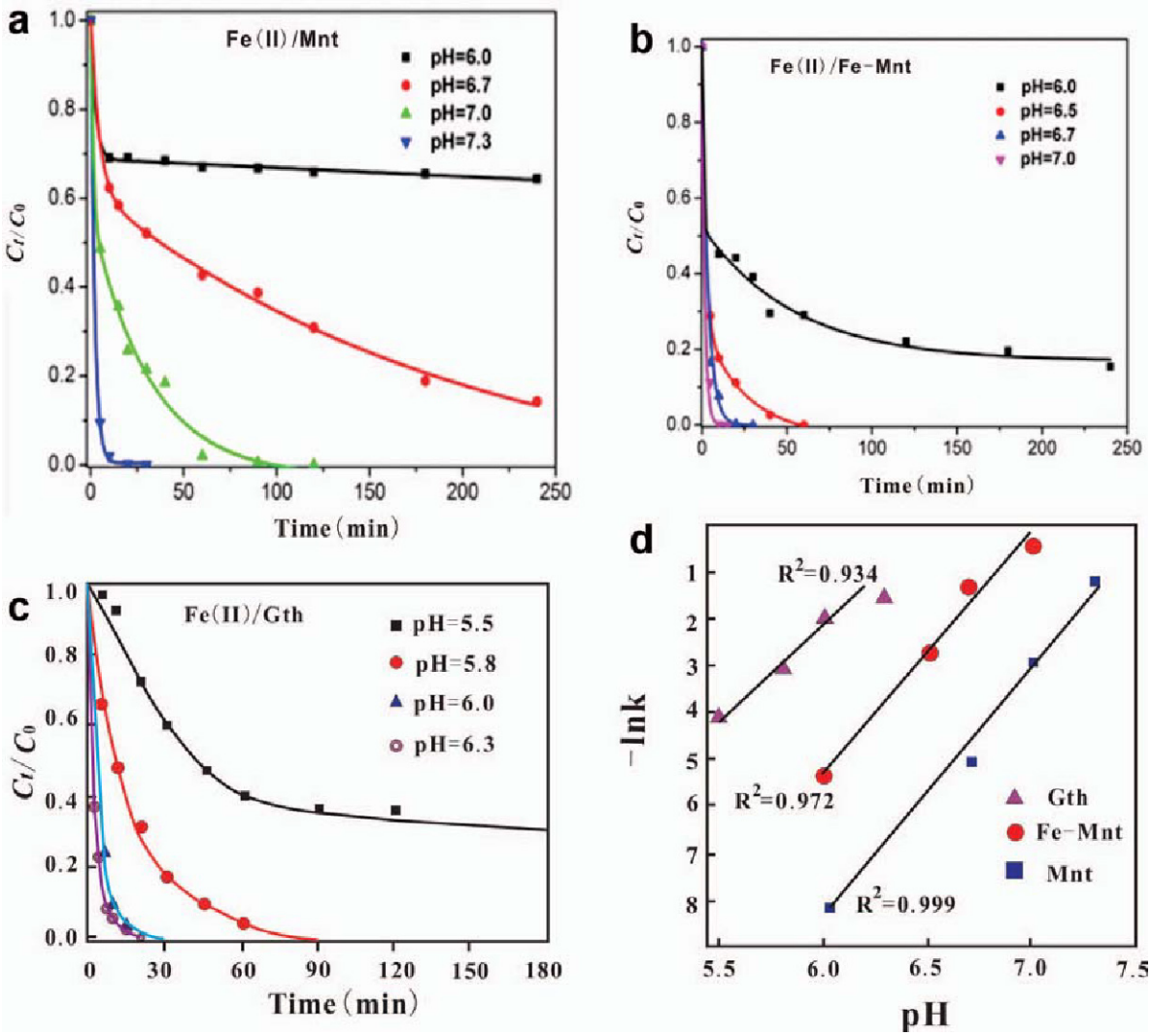

Figure 7. Transformation rate constants (k) of 2-NP at different pHs in (a) Mnt, (b) Fe-Mnt, (c) goethite systems, and (d) plot of k *vs.* pH with initial conditions of 22 μM 2-NP, 4.0 g/L of each catalyst, 0.2 M NaCl, 28 mM MOPS, 3.0 mM Fe(II), and 25°C.

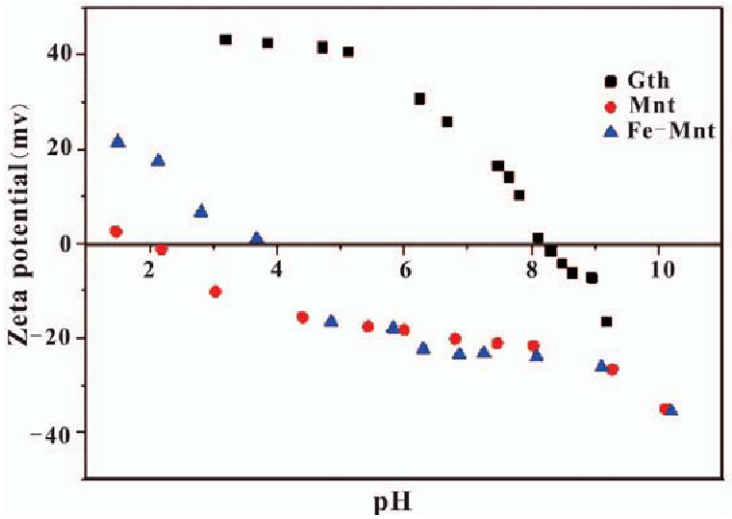

Figure 8. Zeta potentials of Mnt, Fe-Mnt, and goethite *vs.* pH.

https://doi.org/10.1346/CCMN.2018.064107 Published online by Cambridge University Press

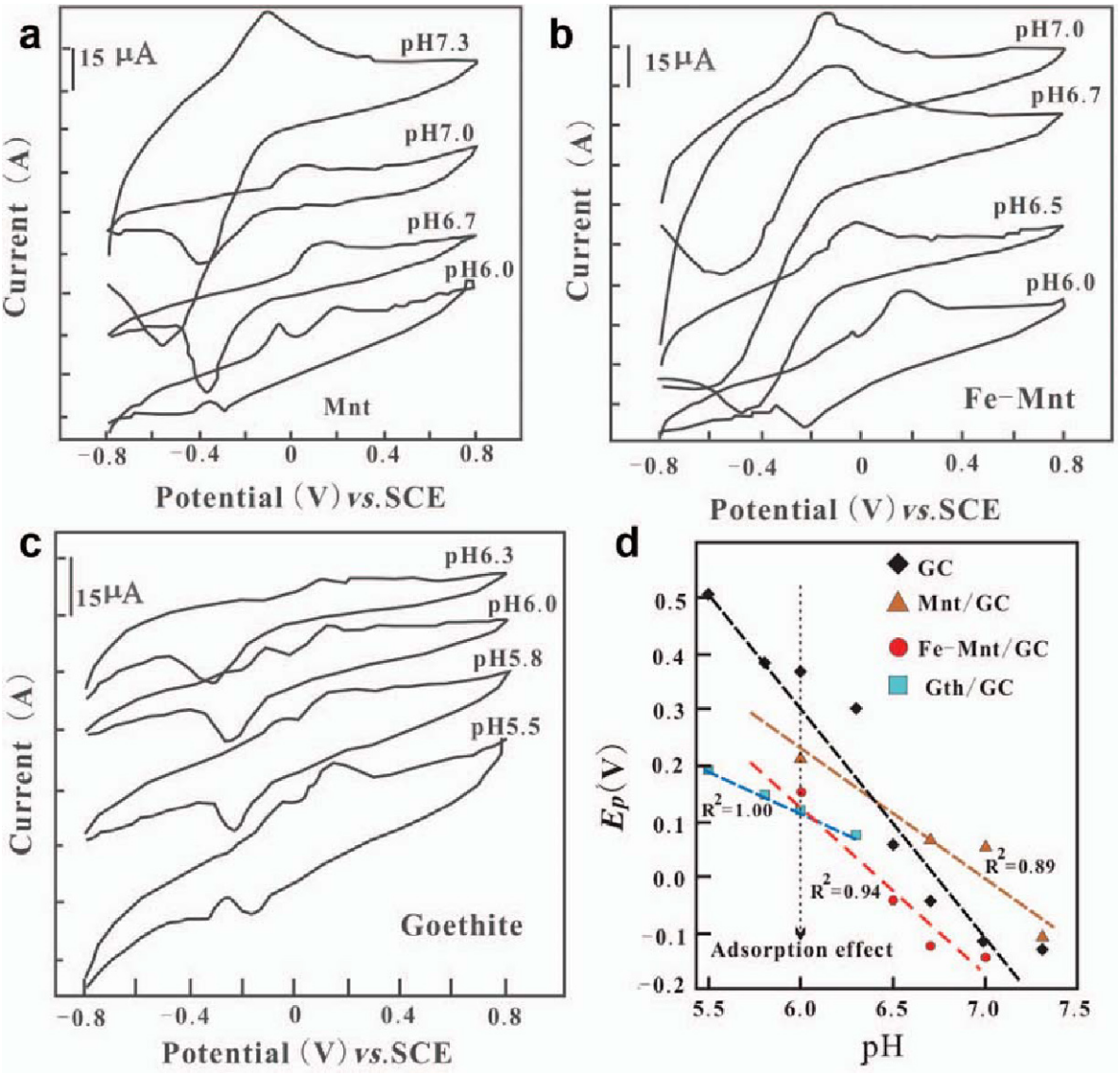

Figure 9. Cyclic voltammograms of Fe(II) adsorbed to (a) Mnt/GC, (b) Fe-Mnt/GC, (c) Gth/GC, and (d) plot of E_P *vs.* pH; GC = the bare glassy C electrode.. The test conditions were 3.0 mM $FeSO_4$, 0.2 M NaCl, 28 mM buffer, and 25ºC.

potentials (denoted E_P) and the kinetic rate constants (k) under various conditions (Table 3) revealed that the measured E_P values for Mnt/GC, Fe-Mnt/GC, and Gth/GC at pH 6.0 were 0.210, 0.190, and 0.125 V, respectively. The trends in the changes of E_p reduction values with pH were the same among the three minerals, but the change in E_p reduction values for goethite were greater in the low pH range (Figure 9).

When the pH was changed from 6.0 to 6.7, however, the E_p values of Fe(II) adsorbed to Fe-Mnt decreased from 0.190 to −0.118 V, while the E_p values for Mnt decreased from 0.210 to 0.099 V. The corresponding 2-NP removal efficiencies by Fe-Mnt were higher than those for Mnt. This electrochemical evidence proves that the E_p values of the Fe(II) surface complex species can be remarkably affected by the pH. It also indicated that the enhanced reduction of 2-NP was related to the reduced E_P values of the Fe(II) surface complex, *e.g.* the E_p value reached −0.107 V for Mnt at pH 7.3.

Linear relationships between E_p values and pH were clearly observed for Mnt and Fe-Mnt at pHs >6.0, but that relationship for goethite can be observed at any pH (Figure 9d). The relationships for Mnt and Fe-Mnt can be ascribed to the predominant adsorption of Fe(II) to Mnt and Fe-Mnt at pHs of ⩽6.0 by cation exchange, which resulted in higher E_p values and nearly no reduction occurred because the Fe(II) surface complex with Mnt and Fe-Mnt was almost negligible in the low pH range.

The decrease in E_P values was more evident in the high pH range (>6.5) for Mnt and Fe-Mnt. The Fe(II)

https://doi.org/10.1346/CCMN.2018.064107 Published online by Cambridge University Press

Table 3. Rate constants (k) and peak oxidation potentials (E_p) under various conditions. The bold numbers highlight the k, E_p, and R^2 values at pH 6.0.

Work electrodes	Variations in pH	Constant conditions	E_p (V)	k (min^{-1})	R^2
GC	**6.0**	$[Fe^{2+}]$ = 3.0 mM, T = 25ºC, and [NaCl] = 0.2 M	**0.369**	**0.002**	**0.967**
	6.5		0.065	0.008	0.974
Mnt/GC	**6.0**	[Mnt] = 4.0 g/L, $[Fe^{2+}]$ = 3.0 mM, T = 25ºC, and [NaCl] = 0.2 M	**0.210**	**0.000**	**0.924**
	6.7		0.099	0.007	0.993
	7.0		0.056	0.056	0.952
	7.3		−0.107	0.314	0.977
Fe-Mnt/GC	**6.0**	[Fe-Mnt2] = 4.0 g/L, $[Fe^{2+}]$ = 3.0 mM, T = 25ºC, and [NaCl] = 0.2 M	**0.155**	**0.005**	**0.908**
	6.5		−0.036	0.066	0.992
	6.7		−0.118	0.271	0.977
	7.0		−0.137	0.623	0.972
Gth/GC	5.5	[Gth] = 4.0 g/L, $[Fe^{2+}]$ = 3.0 mM, T = 25ºC, and [NaCl] = 0.2 M	0.190	0.016	0.983
	5.8		0.152	0.045	0.993
	6.0		**0.125**	**0.176**	**0.976**
	6.3		0.085	0.224	0.987

complexation to oxides can be strengthened at pHs $\geqslant$7.0 (Li *et al*., 2009). Thus, the 2-NP reductive removal enhanced by Mnt and Fe-Mnt at pHs >7.0 may be attributed to the increased amounts of Fe(II) surface complex species bound to the edges and/or even to polyhydroxyl-Fe oxide surfaces. Even though the amounts of both $FeOH^+$ and Fe^{2+} species of adsorbed Fe(II) increased with higher pHs (Danielsen and Hayes, 2004), the $\equiv FeOFeOH^0$ species was predominant over $\equiv FeOFe^+$ in the high pH range.

Linear relationships between ln k and solution pH were also observed for the three systems (Figure 7d). Due to polyhydroxyl-Fe oxide introduced into the Mnt particles, the Fe-Mnt k values were greater than the Mnt values. The E_p values for Fe-Mnt decreased remarkably (Table 3), and thus endowed Fe-Mnt with a higher catalytic ability than Mnt. This may be ascribed to the presence of $\equiv FeOFeOH^0$ rather than $\equiv FeOFe^+$ on Fe-Mnt. Goethite forms many more surface $\equiv FeOFe^+$ sites in the low pH range. A previous study reported a trend of enhanced k values for 2-NP removal under the same conditions in the order of γ-FeOOH > α-FeOOH > α-Fe_2O_3 (Tao *et al*., 2010).

Recycling of Fe-Mnt

To examine the reusability of Fe-Mnt, reusability experiments were conducted using the same catalyst 3 times after it was regenerated *via* sonication and washing with deionized water. After recycling 3 times, the Fe-Mnt sample maintained an efficient catalytic activity (Figure 10). As seen in Figure 10, the surface catalytic activity of the regenerated Fe-Mnt was even slightly increased in the subsequent catalysis runs by the precipitation of newly produced Fe(III).

Possible mechanisms of enhanced 2-nitrophenol reduction

Polyhydroxyl-Fe(III) pillaring into Mnt particles can alter the external and internal surface properties. The amount of the Fe(II) surface complex adsorbed onto Fe-Mnt was much higher than that for the untreated Mnt at the same pH. The enhanced surface complexation can promote the reductive catalytic activity of Fe-Mnt.

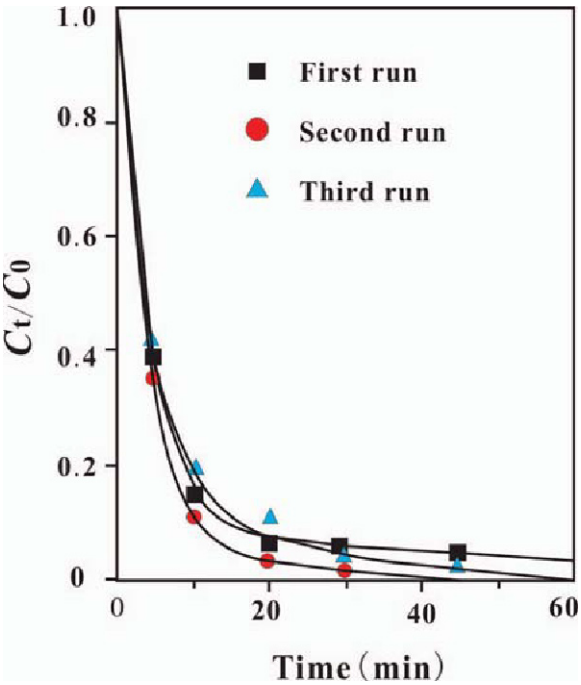

Figure 10. Efficacy of 2-NP reduction by recycled Fe-Mnt samples under the initial conditions of 22 μM 2-NP, 4.0 g/L Fe-Mnt, 3.0 mM Fe(II), pH = 6.5, and 25ºC.

https://doi.org/10.1346/CCMN.2018.064107 Published online by Cambridge University Press

Hence, surface catalysis can effectively improve the Fe(II) reductive activity, which is related to a negative shift in the redox potential of adsorbed Fe(II) species (Tao and Li, 2012). The more positive redox potential (E_h) corresponds to the greater affinity of the species for electrons and a stronger tendency to be reduced. The E_h of the surface associated Fe(II) species decreased after mineral surface catalysis. This means that the chemically adsorbed Fe(II) species give rise to easy electronic transfer to mineral surfaces. Apparently, Fe(II) surface complex species can be an excellent reductant. For instance, the measured reduction potential of Fe(III)/goethite at pH 6.3 decreased to -0.3 V in the present work, while it decreased to less than -0.6 V at pH 7.0 (Borch *et al*., 2010). Similar to the Fe(III)/goethite, the reduction potential of Fe(III)/Fe-Mnt also decreased to -0.6 V at pH 7.0 (Figure 9b).

The trends in the oxidation potential (E_p) of the adsorbed Fe(II) species, however, were remarkably different among the three mineral materials as described in detail above. This indicated a large variation in the enhanced reactivity of Fe(II). This variation can be attributed to the different modes of Fe(II) adsorption by the three mineral materials, which were cation exchange of Fe(II) by Mnt, surface complexation of Fe(II) by goethite, and cation exchange and surface complexation of Fe(II) by Fe-Mnt. As a result, the potential mechanisms responsible for the enhanced 2-NP reduction by Fe-Mnt are described below.

All 2-NP reductive transformation processes followed the pseudo first-order kinetics given by equation 2 below with an $R^2 > 0.98$ and kinetics rate constants that increased with increases in pH. This clearly demonstrated that the Fe(II) species related to the surface complex should be the dependent factor, but that interfacial diffusion of reactants to mineral surfaces was a factor that can affect the Fe(II) surface complex generation rate (Wei *et al.*, 2017).

$$\ln(C_t/C_0) = -kt \quad (2)$$

The adsorption capacity of the surface-complex Fe(II) species can significantly mediate the reductive ability of Fe(II) species to reductively transform 2-NP. Even though the specific surface area of Fe-Mnt was obviously increased, the surfaces of Mnt particles in Fe-Mnt were not fully covered by the added Fe-oxides and resulted in a reductive catalytic activity of Fe-Mnt that did not exceed that of goethite, but was much better than Mnt. The final product of the reductive transformation of 2-NP was 2-aminophenol (2-AP) (equations 3–6), but possible intermediate compounds were not determined in this work.

$$Fe(II)^{2+} + \equiv SOH^0 \text{ (mineral surfaces)} \rightarrow \equiv SOFe(II)^{+} + H^{+} \quad (3)$$

$$Fe(II)OH^{+} + \equiv SOH^0 \rightarrow \equiv SOFe(II)OH^0 + H^{+} \quad (4)$$

$$\equiv SOFe(II)^{+} + \text{2-nitrophenol} \rightarrow \equiv SOFe(III)^{2+} + \text{2-aminophenol} \quad (5)$$

$$\equiv SOFe(II)OH^0 + \text{2-nitrophenol} \rightarrow \equiv SOFe(III)OH^{+} + \text{2-aminophenol} \quad (6)$$

CONCLUSIONS

This study demonstrated that the introduction of polyhydroxyl-Fe into montmorillonite exhibited a remarkable effect in enhancing the ability of Fe(II) to reduce 2-NP. The synthetic Fe-Mnt has an enhanced surface reductive catalytic activity that results in the reduction of 2-NP by a Fe(II)/Fe-Mnt mixed system, which is more efficient than the Fe(II)/Mnt mixed system. The enhanced rates for 2-NP removal from a Fe(II)/Fe-Mnt mixed system can be ascribed to the important contribution of specifically adsorbed Fe(II) bound to the surface hydroxyls of Fe-Mnt. Due to polyhydroxyl-Fe(III) introduction into Mnt, the Fe-Mnt that formed evidently increased the adsorption capacity for the Fe(II) surface complex species. The amount of Fe(II) surface complex sites increased with increased pH. Therefore, a direct pH increase and/or polyhydroxyl-Fe(III) introduction into Mnt can both significantly increase the amounts of the Fe(II) surface complex adsorbed to Fe-Mnt. Furthermore, the Fe(II) surface complex can effectively enhance 2-NP transformation. As a result, the above two measures can significantly improve 2-NP reduction efficiency.

ACKNOWLEDGMENTS

Financial support for this project came from the National Natural Science Foundation of China (No. 41372050) and Guangdong Provincial Natural Science Foundation (No. 2018B030311021).

REFERENCES

Borch, T., Inskeep, W.P., Harwood, J.A., and Gerlach, R. (2005) Impact of ferrihydrite and anthraquinone- 2,6-disulfonate on the reductive transformation of 2,4,6-trinitrotoluene by a gram-positive fermenting bacterium. *Environmental Science & Technology*, **39**, 7126–7133.

Borch, T., Kretzschmar, R., Kappler, A., Van Cappellen, P., Ginder-Vogel, M., Voegelin, A., and Campbell, K. (2010) Biogeochemical redox processes and their impact on contaminant dynamics. *Environmental Science & Technology*, **44**, 15–23.

Brookshaw, D.R., Coker, V.S., Lloyd, J.R., Vaughan, D.J., and Pattrick, R.A.D. (2014) Redox interactions between Cr(VI) and Fe(II) in bioreduced biotite and chlorite. *Environmental Science & Technology*, **48**, 11337–11342.

Brunauer, S., Deming, L.S., Deming, W.E., and Teller, E. (1940) On a theory of the van der Waals adsorption of gases. *Journal of the American Chemical Society*, **62**, 1723–1732.

Dai, S.G. (2006) *Environmental Chemistry*, second edition. Higher Education Press, Beijing, pp. 186.

Danielsen, K.M. and Hayes, K.F. (2004) pH dependence of carbon tetrachloride reductive dechlorination by magnetite. *Environmental Science & Technology*, **38**, 4745–4752.

Elsner, M., Schwarzenbach, R.P., and Haderlein, S.B. (2004)

Reactivity of Fe(II)-bearing minerals towards reductive transformation of organic contaminants. *Environmental Science & Technology*, **38**, 799–807.

Haderlein, S.B. and Schwarzenbach, R.P. (1995) Environmental processes influencing the rate of abiotic reduction of nitroaromatic compounds in the subsurface. Pp. 199–225 in: *Biodegradation of Nitroaromatic Compounds* (J.C. Spain, editor). Plenum, New York.

Hoffstetter, T.B., Heijman, C.G., Haderlein, S.B., Holliger, C., and Schwarzenbach, R.P. (1999) Complete reduction of TNT and other (poly)nitroaromatic compounds under iron-reducing subsurface conditions. *Environmental Science & Technology*, **33**, 1479–1487.

Jones, A.M., Kinsela, A.S., Collins, R.N., and Waite, T.D. (2016) The reduction of 4-chloronitrobenzene by Fe(II)-Fe(III) oxide systems-correlations with reduction potential and inhibition by silicate. *Journal of Hazardous Materials*, **320**, 143–149.

Klausen, J., Trober, S.P., Haderlein, S.B., and Schwarzenbach, R.P. (1995) Reduction of substituted nitrobenzenes by Fe(II) in aqueous mineral suspensions. *Environmental Science & Technology*, **29**, 2396–2404.

Klupinski, T.P., Chin, Y.P., and Traina, S.J. (2004) Abiotic degradation of pentachloronitrobenzene by Fe(II): Reactions on goethite and iron oxide nanoparticles. *Environmental Science & Technology*, **38**, 4353–4360.

Li, F.B., Tao, L., Feng, C.H., Li, X.Z., and Sun, K.W. (2009) Electrochemical evidences for promoted interfacial reactions: The role of adsorbed Fe(II) onto γ-Al_2O_3 and TiO_2 in reductive transformation of 2-Nitrophenol. *Environmental Science & Technology*, **43**, 3656–3661.

Li, F.B., Wang, X.G., Li, Y.T., Liu, C.S., Zeng, F., Zhang, L.J., Hao, M.D., and Ruan, H.D. (2008) Enhancement of the reductive transformation of pentachlorophenol by polycarboxylic acids at the iron oxide-water interface. *Journal of Colloid and Interface Science*, **321**, 332–341.

Pentráková, L., Su, K., Pentrák, M., and Stucki, J.W. (2013) A review of microbial redox interactions with structural Fe in clay minerals. *Clay Minerals*, **48**, 543–560.

Schultz, C.A. and Grundl, T.J. (2000) pH dependence on reduction rate of 4-Cl-nitrobenzene by Fe(II)/montmorillonite systems. *Environmental Science & Technology*, **34**, 3641–3648.

Strathmann, T.J. and Stone, A.T. (2002) Reduction of oxamyl and related pesticides by Fe(II): Influence of organic ligands and natural organic matter. *Environmental Science & Technology*, **36**, 5172–5183.

Stumm, W. and Sulzberger, B. (1992) The cycling of iron in natural environments: Considerations based on laboratory studies of heterogeneous redox processes. *Geochimica et Cosmochimica Acta*, **56**, 3233–3257.

Tao, L. and Li, F.B. (2012) Electrochemical evidence of Fe(II)/Cu(II) interaction on titanium oxide for 2-nitrophenol reductive transformation. *Applied Clay Science*, **64**, 84–89.

Tao, L., Li, F.B., Wang, Y.K., and Sun, K.W. (2010) Reductive activity of adsorbed Fe(II) on iron (oxyhydr) oxides for 2-nitrophenol transformation. *Clays and Clay Minerals*, **58**, 682–690.

Tao, L., Zhang, W., Li, H., Li, F.B., Yu, W.M., and Chen, M.J. (2012) Effect of pH and weathering indices on the reductive transformation of 2-nitrophenol in South China. *Soil Science Society of America Journal*, **76**, 1579–1591.

Wei, X.P., Wu, H.H., He, G.P., and Guan, Y.F. (2017) Efficient degradation of phenol using iron-montmorillonite as a Fenton catalyst: Importance of visible light irradiation and intermediates. *Journal of Hazardous Materials*, **321**, 408–416.

Wu, H.H., Dou, X.W., Deng, D.Y., Guan, Y.F., Zhang, L.G., and He, G.P. (2012) Decolourization of the azo dye Orange G in aqueous solution *via* a heterogeneous Fenton-like reaction catalysed by goethite. *Environmental Technology*, **33**, 1545–1552.

Wu, H.H., Xie, H.R., He, G.P., Guan, Y.F., and Zhang, Y.L. (2016) Effects of the pH and anions on the adsorption of tetracycline on iron-montmorillonite. *Applied Clay Science*, **119**, 161–169.

Yuan, P., Bergaya, F., Tao Q., Fan, M., Liu, Z., Zhu, J., He, H., and Chen, T. (2008) A combined study by XRD, FTIR, TG and HRTEM on the structure of delaminated Fe-intercalated/pillared clay. *Journal of Colloid and Interface Science*, **324**, 142–149.

Zhang, J.H., Wei, G.L., Li, Y., Liang, X.L., Chu, W., He, H.P., Huang, D.Y., Zhu, J.X., and Zhu, R.L. (2017) Reduction removal of hexavalent chromium by zinc-substituted magnetite coupled with aqueous Fe(II) at neutral pH value. *Journal of Colloid and Interface Science*, **500**, 20–29.

(*Received 11 October 2017; revised 17 July 2018; Ms. 1216; AE: Chun-Hui Zhou*)